

Flexible Analog-to-Feature Converter for Wireless Smart Healthcare Sensors

Mikhail Manokhin, Paul Chollet, Patricia Desgreys

C2S Team, ComElec Dept., *LTCI, Télécom Paris, Institut Polytechnique de Paris*, Palaiseau, France

emails: {mikhail.manokhin; pachollet; patricia.desgreys}@telecom-paris.fr

Abstract—Analog-to-Feature (A2F) conversion based on Non-Uniform Wavelet Sampling (NUWS) has demonstrated the ability to drastically reduce the energy consumption in wireless sensors while employed for electrocardiogram (ECG) anomaly detection. The underlying idea is to extract relevant features from the analog signal and perform the classification in the digital domain. We adopt the same approach for a human activity recognition (HAR) task, considered as a second application for a proposed generic A2F converter. By extracting only 16 features from the inertial signals of the UCI-HAR data set and using these features as inputs for a simple Neural Network, we achieved an 87.7% accuracy in multiclass classification. From the simulation results, we defined the relevant features and the hardware specifications required for a complete circuit design and chip fabrication.

Index Terms—Analog-to-Feature converter, Smart sensors, Non-Uniform Wavelet Sampling, Human activity recognition.

I. INTRODUCTION

Increasing wireless smart sensors' autonomy is one of the most challenging and necessary tasks in the context of new Internet of Things (IoT) and Wireless Sensor Networks (WSN) applications. The energy used to transmit samples acquired at the Nyquist rate constitutes a significant part of the sensor's total consumption budget. Hence, it reveals crucial to reduce the amount of data sent from the sensor to the aggregator. For this purpose, a compressive sensing (CS) technique for Analog-to-Information (A2I) conversion has been proposed [1]. However, it has a limited compression ratio and needs to perform a full signal reconstruction, which is useless in specific applications and requires complex sparse recovery algorithms [2]. In contrast, Analog-to-Feature (A2F) conversion further reduces the amount of transmitted data by extracting only useful features from the analog signal [3] and using them as inputs for Machine Learning (ML) algorithms for further classification at the sensor or aggregator level.

This work aims to design a generic, reconfigurable A2F converter for various low-frequency signals. A2F conversion based on Non-Uniform Wavelet Sampling (NUWS) [4] has already been proposed for binary arrhythmia detection in ECG signals in [5], showing benefits over the A2I approach and conventional sampling in terms of energy consumption. Herein we adopt arrhythmia detection as the first application and use the same methodology to build a classification model. The ML algorithms were reimplemented using Python and TensorFlow library instead of MATLAB® tools, allowing for more efficient ML models, especially Neural Networks (NNs), and accelerated calculations on graphics processing units.

With the intensive development of IoT, the widespread edge devices equipped with inertial sensors have provided researchers with collections of raw physiological signals for analyzing simple or complex human activities [6]. Human activity recognition (HAR) based on this data has recently gained a strong research interest due to a rapidly increasing demand for various human-centric applications, including health monitoring, sports tracking, smart homes, and human-machine interaction [7], [8]. Traditional ML approaches, i.e., decision trees [9], [10] and support vector machines [11], have already achieved impressive results (more than 94% of accuracy) in HAR. Nevertheless, deep learning techniques [12], especially convolutional neural network (CNN) models, avoiding hand-crafted feature extraction [13], [14], have become dominant in this field. Being a typical pattern recognition task, HAR is well suited as a second application to demonstrate the genericity of the proposed A2F converter, which extracts only a few useful features to reduce the amount of transmitted data, thus making the use of CNN redundant. With the help of HAR simulation results and those of ECG arrhythmia detection, we will define the relevant features for extraction and the system's parameters necessary for the complete circuit design and chip fabrication.

The main contributions of this paper are: (1) HAR simulations for the generic A2F converter with NUWS-based feature extraction, (2) determination of the relevant features and the hardware specifications for the converter's implementation.

The rest of the paper is organized as follows. In section II, we briefly introduce the architecture of the proposed A2F converter, the details of NUWS-based feature extraction, and the 2-stage feature selection. Section III presents a setup and simulation results of ECG arrhythmia detection and HAR. Section IV deduces the specifications required for a complete A2F converter's circuit design from the simulation results. Finally, we summarize our conclusions in section V.

II. ANALOG-TO-FEATURE CONVERSION

The architecture of the proposed acquisition system containing the generic and reconfigurable A2F converter [15] is shown in Fig. 1. It performs the following operations:

- extraction of NUWS-based analog domain features [4]
- analog-to-digital conversion of extracted features
- application-specific binary or multiclass classification
- context detection, which activates the required feature extractors and configures their internal wavelet generators, depending on the application or desired precision.

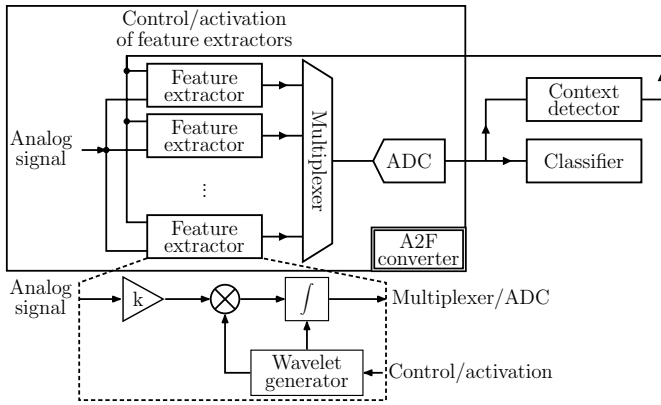


Fig. 1. Architecture of the acquisition system with the reconfigurable A2F NUWS-based converter

For the extraction of NUWS-based features, the analog signal is mixed with tunable wavelets (WLs) and then integrated within the analysis window. Figure 2 illustrates the examples of Haar and Gabor WLs, the two families of WLs used in this work. Haar WLs represent the square functions taking values ± 1 and 0 , while Gabor WLs are the product of a complex exponential with a Gaussian window. One of the main advantages of the NUWS is that it allows for obtaining temporal and frequency information of the input signal simultaneously. It provides several degrees of freedom during a WL generation: its oscillation frequency, support size, and temporal position in the analysis window. Thus, the number of possible WLs, i.e., features, is enormous, which makes a proper feature selection process necessary to determine a reduced set of relevant features required for a given classification task.

Following the adopted methodology [5], a combination of two feature selection algorithms is applied during simulations. Firstly, only the 100 best features are chosen according to the Information Gain (IG) criterion without building an ML model. It considerably reduces the time to perform the following selection step, Sequential Forward Search (SFS), which scales quadratically with the number of features. It evaluates the classification performances of NN classifiers built with different subsets of these features as inputs. The features leading to the highest value of a classification metric are gradually added to the set, which is initially empty. A new NN classifier is trained and evaluated for each new subset.

The basic SFS algorithm, maximizing the classification accuracy, can be modified to account for the A2F converter's

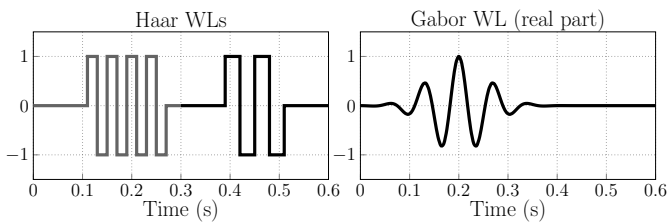


Fig. 2. Examples of Haar and Gabor wavelets

hardware complexity and power consumption. First of all, as each extractor is capable of extracting multiple features that do not superpose in the analysis window (e.g., produced by two Haar WLs from Fig. 2), it is possible to limit the maximum number of parallel extractors. The resulting algorithm is called the adapted SFS. The optimized SFS algorithm, in addition to this, takes into account the energetic cost during the extraction of each feature to minimize the total energy consumption while maximizing the classification accuracy.

III. SIMULATION RESULTS

A. Arrhythmia detection

Thanks to more advanced software used, the reproduced simulation results of binary arrhythmia detection in ECG signals are slightly better than those shown in [5]. The optimized SFS algorithm limited to three parallel feature extractors achieves a 98.17% classification accuracy with eight extracted features and $2.6 \mu\text{J}$ energy consumption, whereas $3.35 \mu\text{J}$ were previously required to extract 10 features for a 98% accuracy. The setup details for these simulations are given in Table I. As indicated, only Haar WLs are used, reducing the digital WL generator's complexity and allowing the deployment of a simple mixer, with negligible loss in classification accuracy in contrast to Gabor WLs. These similar results validate the new simulator that can be used for a second application of the proposed A2F converter in the form of HAR.

B. Human activity recognition

In contrast to arrhythmia detection, HAR has been explored for both multiclass and binary classifications of Activities of Daily Living (ADL). Also, as shown in Table I, the NUWS exploited Haar and complex-valued Gabor WLs.

Since static activities (sitting, standing, and laying) are represented by constant values of acceleration and angular velocity, the integration of such signals with any WLs (zero average functions by definition) results in zero. Thus, a "constant" WL, equal to one in the whole analysis window, has been added to the Haar WL dictionary. Otherwise, the confusion between static activities is significant, abruptly reducing the overall classification accuracy. Moreover, this "constant" WL does not require the use of the WL generator, as the feature produced by it results from a raw signal integration, which gives a value proportional to a signal's average.

1) *Multiclass classification*: The performances of multiclass HAR with basic SFS are shown in Fig. 3. The accuracy is plotted against the number of selected features. The simulations for Haar WLs have been conducted with three simple structures of NN classifier: one hidden layer of 10 neurons, two layers of 10 neurons, and one layer of 20 neurons. Then the best classifier's structure has also been tested with Gabor WLs, which require more complex hardware for generation and usually outperform Haar WLs but provide a significantly lower classification accuracy here. The preferable configuration (Haar WLs, NN classifier with one hidden layer of 20 neurons) achieves 88.1% accuracy with 17 features extracted by 10 extractors. Performing the

TABLE I
SETUP FOR SIMULATIONS

	Arrhythmia detection	HAR
Database (signals)	MIT-BIH Arrhythmia [16] (single channel from 48 ECG recordings of 30 min each, sampled at 360 Hz)	UCI-HAR [17] (3-axial acceleration and angular velocity signals from a waist-mounted smartphone, sampled at 50 Hz)
Classes	2 (normal, abnormal)	6 (walking, upstairs, downstairs, sitting, standing and laying)
Type of features	NUWS with Haar WLS	NUWS with Haar or Gabor WLS (generated for all 6 signals)
Feature selection	IG + SFS (optimized)	IG + SFS (basic, adapted)
Type of learning	supervised learning with a 70/30% proportion between learning and test sets	
Analysis window	256 samples of one annotated heartbeat segment (R-peak located at 100th sample) => 0.711 s	128 samples of one annotated ADL segment (50% overlap with adjacent segments) => 2.56 s
Classifier	NN binary classifier (1 hidden layer of 10 neurons, Adam optimizer) trained during 1500 epochs	NN binary or multiclass classifier (1 or 2 hidden layers of 10 or 20 neurons, Adam optimizer) trained during 1500 epochs

multiclass HAR for the same configuration with adapted SFS (limit of parallel extractors) leads to the results given in Fig. 4 for four different values of a maximum number of extractors $nExt_{max}$. For each curve, the square marker shows the point when the maximum number of extractors is reached. As seen, the curve with $nExt_{max} = 10$ attains lower accuracy (87.8% with 15 features) than basic SFS with the same number of extractors in the trade-off point mentioned above. This is caused by a random initialization of parameters during a NN classifier's training, affecting each evaluated feature subset's performance and subsequent choice of the relevant features. Moreover, the converter with the number of extractors reduced to eight achieves a slightly lower classification accuracy of 87.7% (round marker) by extracting 16 features. An analysis of the selected features showed that among all six available signals, only two axes of acceleration and one axis of angular velocity are needed to produce the WLS required in this case.

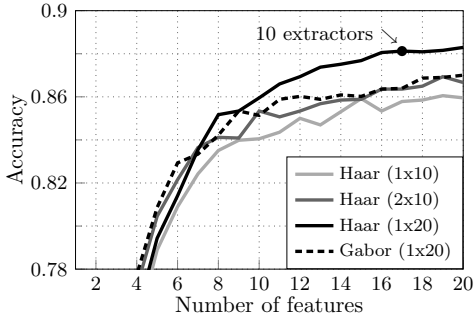


Fig. 3. Performances of multiclass HAR with basic SFS

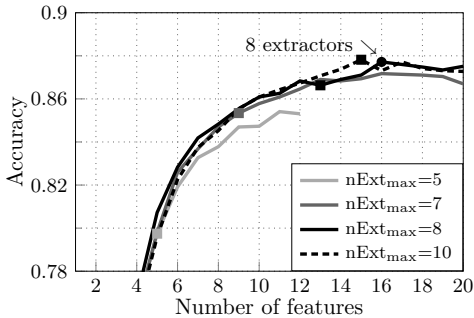


Fig. 4. Performances of multiclass HAR with adapted SFS

2) *One-vs-all binary classification*: The Matthews correlation coefficient (MCC) is known to be more informative than the accuracy in evaluating binary classification problems [18]. The reason is that MCC takes into account the size of the four categories of the confusion matrix (true positives TP , true negatives TN , false positives FP , false negatives FN) and is given by:

$$MCC = \frac{TP \cdot TN - FP \cdot FN}{\sqrt{(TP+FP)(TP+FN)(TN+FP)(TN+FN)}} \quad (1)$$

This advantage is especially prominent in the case of imbalanced data sets. This condition is particularly true for one-vs-all binary classification performed here with the UCI-HAR data. Occurrences of each class in this data set are almost equal, making it balanced only for the multiclass classification.

The performances of binary HAR with adapted SFS are depicted in Fig. 5, where the same configuration with Haar WLS and one hidden layer of 20 neurons has been used. Different values of a maximum number of parallel extractors $nExt_{max}$ have been considered, but only the best cases for each classification are shown. Curve markers indicate the trade-off points between the achieved MCC values and the number of required features. Laying activity is not shown in Fig. 5 as it is distinguished perfectly from other activities with the help of only one feature produced by the "constant" WL and the acceleration along the x-axis.

Table II summarizes the best trade-off points from binary and multiclass HAR simulation results. As the relevant features in certain classifications include those produced by the

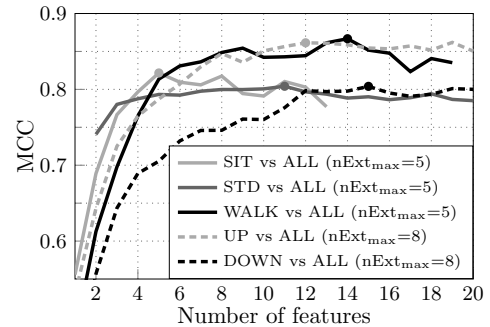


Fig. 5. Performances of one-vs-all binary HAR with adapted SFS

TABLE II
SUMMARY OF HAR SIMULATIONS

Classification	LAY vs ALL	SIT vs ALL	STD vs ALL	WALK vs ALL	UP vs ALL	DOWN vs ALL	Multiclass
N° of features	1	5	11	14	12	15	16
Metric (MCC/Accuracy*)	1.0	0.822	0.804	0.867	0.861	0.804	0.877*
N° of extractors	1	4	5	5	8	7	8
N° of WL generators	0	2	4	4	7	7	6

TABLE III
COMPARISON OF MULTICLASS HAR PERFORMANCES

Model	Accuracy	Input size	Parameters
CNN [14]	96.98%	1152	0.342M
CNN [19]	97.21%	(9x128:	0.45M
CNN [20]	96.98%	3 axes for	0.35M
CNN [21]	91.67%	-acceleration,	0.424M
CNN-LSTM [21]	94.48%	-ang. velocity,	3.5M
vLSTM [21]	90.80%	-acceleration	0.084M
sLSTM [21]	91.82%	w/o gravit.	0.61M
BiLSTM [21]	93.91%	component)	0.168M
iSPLInception [21]	95.09%		1.33M
This work: Feedforward NN (1 hidden layer of 20 neurons)	87.72%	16 (features from 3 signals: acc_x, acc_y, gyr_z)	466

”constant” WL, the number of WL generators is less than the number of required feature extractors. The multiclass HAR classification is preferred over its binary counterpart because it is more common in the HAR domain and completes the distinction of all activities with one NN and fewer features, extractors, and WL generators. In contrast, to distinguish all six activities from each other in a binary way, six different NNs with 58 features in total would be required.

Table III compares the performances of the different models from the literature with the results we obtained for the multiclass HAR on the UCI-HAR data set. Although our classifier provides a lower accuracy, it requires at least hundreds of times fewer parameters and a much smaller input size. Such a simple artificial NN with a digital architecture can be implemented at a sensor level to reduce further the sensor’s consumption by sending only the classification results. Moreover, memristors-based analog, reconfigurable NN [22] will allow digitizing only the classifier’s decision and also being able to adapt to the application or context.

IV. SPECIFICATIONS FOR A HARDWARE IMPLEMENTATION

Based on the obtained results, for the A2F converter to be suitable for both applications, it should consist of eight parallel extractors: three are enough for ECG arrhythmia detection, and all eight are needed for multiclass HAR (two of them without a WL generator). The configuration of WLs will be stored in memory blocks of digital WL generators, which also have to provide a programmable clock signal with databases’ sampling frequencies (50 Hz or 360 Hz).

Using Haar WLs reduces the digital WL generator’s complexity and simplifies a mixer’s schematic to four CMOS transmission gates in the case of the differential amplification stage. To process at least two types of signals, the amplification stage

requires a variable gain. Hence, it should be composed of a low noise amplifier (LNA) and a programmable gain amplifier (PGA), e.g., from a bio-sensing front-end circuit [23]. The integrator, which is essentially a first-order LPF, requires a cut-off frequency much lower than the minimum frequency of a signal to be integrated, i.e., $F_{min} \ll 1/2.56\text{s} = 0.39\text{Hz}$ (two samples in the analysis window of HAR). Besides the multiplexer providing the values for an ADC, the feature extractors should be equipped with multiplexers to select the inertial signals before amplification during the HAR task.

So far, all the simulations have been executed on floating point double precision 64-bit data. However, the extracted analog features are digitized by an ADC to reduce the amount of data used for further classification either at the sensor level or after transmission to an aggregator. In the case of ECG arrhythmia detection, 6-bit precision appeared to be enough to maintain the same classification accuracy while performing the feature selection by the SFS on digitized data [5]. Similar studies should be performed for HAR to determine the ADC specifications. In terms of speed, the highest conversion rate will not exceed the databases’ sampling frequencies (50 Hz or 360 Hz). Hence, a 10-bit SAR ADC with a 40 kHz maximum sampling frequency [23] will probably meet the requirements.

V. CONCLUSION

In this paper, we worked on designing a generic, reconfigurable A2F converter capable of extracting only relevant features from different low-frequency analog signals and performing the corresponding classification tasks in the digital domain, either at the sensor or aggregator level. NUWS-based converter’s architecture has previously shown its efficiency over other acquisition approaches in terms of power consumption and hardware complexity while employed for ECG arrhythmia detection. We adopted the same classification methodology but reimplemented the ML algorithms with more advanced software to carry out the simulations for arrhythmia detection, as well as for a newly proposed HAR application to prove the converter’s genericity. In particular, by extracting only 16 features from the acceleration and angular velocity signals of the UCI-HAR data set with the help of eight parallel extractors and using these features as inputs for a simple NN classifier, we achieved an 87.7% multiclass classification accuracy. The simulation results of both applications allowed us to determine the relevant features for extraction and the specifications for a physical implementation of a whole transmission system incorporating the A2F converter. Future work will focus on the design of a chip and the first physical demonstration of the converter’s performance.

ACKNOWLEDGEMENT

This work was partly carried out in the context of Beyond5G, a project funded by the French government as part of the economic recovery plan, namely "France Relance", and the investments for the future program.

REFERENCES

- [1] E. J. Candes and M. B. Wakin, "An introduction to compressive sampling," *IEEE Signal Processing Magazine*, vol. 25, no. 2, pp. 21–30, 2008.
- [2] E. Crespo Marques, N. Maciel, L. Naviner, H. Cai, and J. Yang, "A review of sparse recovery algorithms," *IEEE Access*, vol. 7, pp. 1300–1322, 2019.
- [3] B. Rumberg, D. W. Graham, V. Kulathumani, and R. Fernandez, "Hibernets: energy-efficient sensor networks using analog signal processing," *IEEE Journal on Emerging and Selected Topics in Circuits and Systems*, vol. 1, no. 3, pp. 321–334, 2011.
- [4] M. Pelissier and C. Studer, "Non-uniform wavelet sampling for RF Analog-to-Information conversion," *IEEE Transactions on Circuits and Systems I: Regular Papers*, vol. 65, no. 2, pp. 471–484, 2018.
- [5] A. Back, P. Chollet, O. Fercoq, and P. Desgreys, "Power-aware feature selection for optimized Analog-to-Feature converter," *Microelectronics Journal*, vol. 122, p. 105386, 2022. [Online]. Available: <https://www.sciencedirect.com/science/article/pii/S002626922200026X>
- [6] J. Sena, J. Barreto, C. Caetano, G. Cramer, and W. R. Schwartz, "Human activity recognition based on smartphone and wearable sensors using multiscale dcnn ensemble," *Neurocomputing*, vol. 444, pp. 226–243, 2021.
- [7] M. Abdel-Basset, H. Hawash, V. Chang, R. K. Chakraborty, and M. Ryan, "Deep learning for heterogeneous human activity recognition in complex IoT applications," *IEEE Internet of Things Journal*, vol. 9, no. 8, pp. 5653–5665, 2022.
- [8] M. A. A. Al-qaness, A. Dahou, M. A. Elaziz, and A. M. Helmi, "Multi-ResAtt: Multilevel residual network with attention for human activity recognition using wearable sensors," *IEEE Transactions on Industrial Informatics*, vol. 19, no. 1, pp. 144–152, 2023.
- [9] P. Casale, O. Pujol, and P. Radeva, "Human activity recognition from accelerometer data using a wearable device," in *Pattern Recognition and Image Analysis*. Berlin, Germany: Springer, 2011, pp. 289–296.
- [10] V. Radhika, C. Prasad, and A. Chakradhar, "Smartphone-based human activities recognition system using random forest algorithm," in *2022 International Conference for Advancement in Technology (ICONAT)*, 2022, pp. 1–4.
- [11] N. Ahmed, J. I. Rafiq, and M. R. Islam, "Enhanced human activity recognition based on smartphone sensor data using hybrid feature selection model," *Sensors*, vol. 20, no. 1, 2020.
- [12] E. Ramanujam, T. Perumal, and S. Padmavathi, "Human activity recognition with smartphone and wearable sensors using deep learning techniques: A review," *IEEE Sensors Journal*, vol. 21, no. 12, pp. 13 029–13 040, 2021.
- [13] E. Kim, "Interpretable and accurate convolutional neural networks for human activity recognition," *IEEE Transactions on Industrial Informatics*, vol. 16, no. 11, pp. 7190–7198, 2020.
- [14] W. Huang, L. Zhang, W. Gao, F. Min, and J. He, "Shallow convolutional neural networks for human activity recognition using wearable sensors," *IEEE Transactions on Instrumentation and Measurement*, vol. 70, pp. 1–11, 2021.
- [15] M. Verhelst and A. Bahai, "Where analog meets digital: Analog-to-Information conversion and beyond," *IEEE Solid-State Circuits Magazine*, vol. 7, no. 3, pp. 67–80, 2015.
- [16] G. Moody and R. Mark, "The impact of the MIT-BIH arrhythmia database," *IEEE engineering in medicine and biology*, vol. 20, pp. 45–50, 2001.
- [17] D. Anguita, A. Ghio, L. Oneto, X. Parra, and J. L. Reyes-Ortiz, "A public domain dataset for human activity recognition using smartphones," in *21st European Symposium on Artificial Neural Networks, Computational Intelligence and Machine Learning*, Bruges, Belgium, 2013, pp. 437–442.
- [18] D. Chicco and G. Jurman, "The advantages of the Matthews correlation coefficient (MCC) over F1 score and accuracy in binary classification evaluation," *BMC Genomics*, vol. 21, 2020.
- [19] W. Gao, L. Zhang, W. Huang, F. Min, J. He, and A. Song, "Deep neural networks for sensor-based human activity recognition using selective kernel convolution," *IEEE Transactions on Instrumentation and Measurement*, vol. 70, pp. 1–13, 2021.
- [20] Q. Teng, K. Wang, L. Zhang, and J. He, "The layer-wise training convolutional neural networks using local loss for sensor-based human activity recognition," *IEEE Sensors Journal*, vol. 20, no. 13, pp. 7265–7274, 2020.
- [21] M. Ronald, A. Poulouse, and D. S. Han, "iSPLInception: An Inception-ResNet deep learning architecture for human activity recognition," *IEEE Access*, vol. 9, pp. 68 985–69 001, 2021.
- [22] O. Krestinskaya, K. N. Salama, and A. P. James, "Learning in memristive neural network architectures using analog backpropagation circuits," *IEEE Transactions on Circuits and Systems I: Regular Papers*, vol. 66, no. 2, pp. 719–732, 2019.
- [23] H. Bhamra, J. Lynch, M. Ward, and P. Irazoqui, "A noise-power-area optimized biosensing front end for wireless body sensor nodes and medical implantable devices," *IEEE Transactions on Very Large Scale Integration (VLSI) Systems*, vol. 25, no. 10, pp. 2917–2928, 2017.